Coherent Phase-Space Structures Governing Surge Dynamics in Astern Seas

Ioannis Kontolefas, *National Technical University of Athens*, ikon@central.ntua.gr

Kostas J. Spyrou, *National Technical University of Athens*, spyrou@deslab.ntua.gr

ABSTRACT

Consideration of a steep multi-chromatic wave field greatly increases the complexity of ship surge dynamics as it renders the underlying strongly nonlinear system also time-dependent. Consequently, conventional concepts used for the analysis of stationary phase-space flows are no longer sufficient to support an in-depth investigation of ship dynamics. To overcome this hindrance, the concept of hyperbolic Lagrangian Coherent Structures (LCSs) is employed. These phase-space objects can be regarded as finite-time generalizations of the stable and unstable manifolds of hyperbolic trajectories defined in dynamical systems with special (such as periodic or quasiperiodic) time dependencies. LCSs represent, locally, the strongest repelling or attracting material surfaces (curves in the case of 2-dimensional systems) advected with the phase flow. We identify hyperbolic LCSs that are intrinsic to the phase flow associated with the surge motion of a ship in astern seas. To the global approach of LCSs is incorporated a scheme aiming to track in space-time "local features" of the flow. The emerging new toolset can enhance substantially current efforts towards a rigorous assessment of ship dynamic stability in steep following seas.

Keywords: *Surf-riding, Multi-frequency Waves, Lagrangian Coherent Structures*

1. INTRODUCTION

The mechanisms generating surf-riding for a ship in regular seas have been extensively studied in the past (Kan 1990; Spyrou 1996). However, gaining understanding beyond the context of harmonic waves has been considered as a daunting task, till recently. The consideration of a multi-frequency wave field brings in new concepts accruing from the time-dependent nature of the problem.

For the regular sea scenario, it is well known that surf-riding can be identified as an equilibrium solution of the surge equation of motion. The consideration, though, of more general wave forms introduces profound complications. For an irregular seaway, this key definition needs to be revised, since stationary states are not likely to exist; i.e., one cannot assume that the underlying non-autonomous dynamical system will admit constant solutions. Therefore, a broader definition of surf-riding needs to be sought.

These difficulties have been recognized and a phenomenological approach to surf-riding in irregular seas has been proposed, expanding upon the notion of wave celerity and its role in signaling the capture to surf-riding (Spyrou et al. 2012, 2014a). In particular, definition and methods for the calculation of wave celeri-

ty for an irregular seaway were proposed and their relevance to the problem of surf-riding was examined. The appeal of such an approach is that it can permit the evaluation of the probability of surf-riding in irregular seas, by setting up the latter as a threshold exceedance problem.

Through the identification of "surf-riding equilibria", i.e. points on the wave where the equilibrium of forces in the longitudinal direction of the ship is instantaneously satisfied, Belenky et al. (2012) endeavoured to gain insight into the dynamics of surge equation in multi-frequency following waves. It is noted that for the calculation of such points, celerity of irregular waves needs to be evaluated.

In another study, Spyrou et al. (2014b) examined the possibility of extracting and tracking "features" related to the surge dynamics in irregular seas (the term is used to characterize objects that are relevant to the problem considered). It was concluded that meaningful features are found among the elements of the zero set of the "acceleration field" i.e., points on the phase space where the acceleration and its time derivative attain, instantly, zero values. Moreover, it was conjectured that certain points satisfying such a condition correlate with surf-riding events.

In the current work, new methods with potential to yield further insights into the dynamics of the surge motion in multi-chromatic astern seas are applied. In particular, the concept of hyperbolic Lagrangian Coherent Structures (LCSs) is tested for unveiling the changing-in-time organization of system's phase-space. Through their organizing role, these structures can be considered as analogues of the stable and unstable manifolds of hyperbolic fixed points, defined in autonomous dynamical systems. For their identification different methods can be applied. Here, a popular, in the nonlinear dynamics literature, numerical scheme is applied, based on the calculation of the spatial distribution of the largest finite-time Lyapunov Exponent of system's trajectories.

2. LAGRANGIAN COHERENT STRUCTURES

2.1 General

The concept of Lagrangian Coherent Structures seems to have emerged as result of the interbreeding of ideas originating from the fields of dynamical systems theory and fluid dynamics. Although the term was first introduced by Haller & Yuan (2000) many people have contributed in the development of computational strategies – for a short review see Shadden (2011). In the context of fluid flows, LCSs can be physically observed as the cores of emergent trajectory patterns and are identified as, locally, the strongest attracting/repelling material surfaces advected with the flow. LCSs have been extensively used during the last years in a wide range of applications concerning physical and biological flows, while the theory, as well as efficient calculation methods, are still developing.

2.2 Identification of LCSs

Although one can choose among different identification schemes (such as the finite size Lyapunov Exponent (FSLE) approach, or the variational theory of hyperbolic LCSs developed recently by Haller (2011) that enables a more rigorous computation) for the needs of the current study we will consider a widely used computational procedure, which involves the calculation of the largest finite-time Lyapunov Exponent (FTLE) field.

Let us consider the following dynamical system that defines a flow on the plane,

$$\dot{x} = f(x,t), \qquad x \in D \subset \mathbb{R}^2, \quad t \in \left[t^-, t^+\right] \qquad (1)$$

A trajectory of system (1) at time t, starting from the initial condition x_0 at t_0, will be denoted by $x(t;t_0,x_0)$. We can write for the flow map $F_{t_0}^{t}(x_0)$ of (1),

$$\begin{aligned} F_{t_0}^{t}: \quad & D \to D \\ & x_0 \mapsto x(t;t_0,x_0) \end{aligned} \tag{2}$$

Through (2), the phase-particle passing from x_0 at time t_0, is associated with its position $x(t;t_0,x_0)$ at time t. If we furthermore consider two phase-particles, located at x_0 and $x_0+\xi_0$ at time t_0, we can write for their distance $\|\xi_t\|$, in a first order approximation with respect to $\|\xi_0\| \ll 1$,

$$\begin{aligned} \|\xi_t\| &\approx \left\|\nabla F_{t_0}^{t}(x_0)\,\xi_0\right\| = \\ &= \|\xi_0\|\sqrt{\hat{\xi}_0^T\left[\nabla F_{t_0}^{t}(x_0)\right]^T \nabla F_{t_0}^{t}(x_0)\,\hat{\xi}_0} \end{aligned} \tag{3}$$

In the above $\hat{\xi}_0$ is the unit vector along the direction of ξ_0, A^T denotes the transpose of A, while $\nabla F_{t_0}^{t}(x_0)$ is the deformation gradient and $C_{t_0}^{t}(x_0)=\left[\nabla F_{t_0}^{t}(x_0)\right]^T \nabla F_{t_0}^{t}(x_0)$ the right Cauchy-Green deformation tensor, both evaluated at x_0. $C_{t_0}^{t}(x_0)$ is a real symmetric, positive definite tensor and as such has real positive eigenvalues,

$$0 < \lambda_1 \le \lambda_2 \tag{4}$$

Moreover, the corresponding eigenvectors e_i, $i=1,2$ form an orthonormal basis. The Cauchy-Green deformation tensor provides a measure of how line elements in the neighbourhood of x_0 deform under the flow i.e., how the lengths and the angles between line elements change, when considering the configuration in the close vicinity of $x(t;t_0,x_0)$ at times t_0 and t. A circular blob of initial conditions centred at x_0 will evolve into an ellipse, with the major (minor) axis aligned with the direction of the eigenvector e_2 (e_1). The coefficients of expansion along these directions will be given by $\sqrt{\lambda_i}$, $i=1,2$.

The finite-time Lyapunov exponents (FTLEs) are defined as follows,

$$\Lambda_i = \frac{1}{|t-t_0|}\ln\sqrt{\lambda_i}, \qquad i=1,2 \tag{5}$$

The largest FTLE, Λ_2, is usually referred to as "FTLE" without distinction. By virtue of (5) Λ_2 can be regarded as a time-averaged measure of stretching and therefore, as a (rough) measure of a trajectory's hyperbolicity. Yet, as noted by Shadden (2011) and Haller (2011), this does not hold in general.

Through the calculation of the spatial FTLE distribution, the identification of LCSs can be made possible. The latter will appear as local maximizing curves of the FTLE field. Typically, the calculation of the field is performed on the basis of a structured grid of initial conditions spanning a considered domain at a given time t_0. The grid is integrated over a specified time interval, $\tau = t - t_0$, using a numerical integration algorithm. Once the final position of each grid point is calculated, the deformation gradient is obtained by implementing a finite difference scheme on the nodes of the initial grid. In the final step of the procedure, the largest eigenvalue of the deformation gradient is computed and the FTLE field is calculated directly from expression (5). The location of repelling/attracting LCSs can be identified as ridges of the FTLE field when forward/backward integration times are considered – contraction can be viewed as expansion in reverse time.

3. MATHEMATICAL MODEL OF SURGE MOTION

Consider the following unidirectional waveform comprised of N propagating, harmonic wave components,

$$\zeta(x;t) = \sum_{i=1}^{N} A_i \cos\left[k_i x - \omega_i t + \varepsilon_i^{(r)}\right] \tag{6}$$

In the above, x is the distance from an earth-fixed point of reference, while A_i, k_i and ω_i are the amplitude, wave number and frequency, respectively, of the distinct wave component i; $\varepsilon_i^{(r)}$ denotes the random phase of the latter, uniformly distributed in the range $[0, 2\pi)$.

We, furthermore, consider an elementary mathematical model that can reproduce asymmetric surging and surf-riding occurrences in following waves of the form (6) – Spyrou et. al. (2012, 2014a),

$$\underbrace{\left(m - X_{\dot{u}}\right)\ddot{\xi}}_{inertia} = \underbrace{\left(\tau_0 n^2 + \tau_1 n\dot{\xi} + \tau_2 \dot{\xi}^2\right)}_{thrust} - \underbrace{\left(r_1\dot{\xi} + r_2\dot{\xi}^2 + r_3\dot{\xi}^3\right)}_{resistance} + \underbrace{\sum_{i=1}^{N} A_i RAO_i \sin\left[k_i\xi - \omega_i t + \varepsilon_i^{(r)} + \varepsilon_{fi}\right]}_{wave\ force} \tag{7}$$

In the equation above, ξ is the position of a ship-fixed point of reference with respect to the earth-fixed origin, while RAO_i and ε_{fi} denote the response-amplitude-operator and phase, respectively, of the surging force corresponding to the wave component i; n corresponds to the propeller revolutions. The overdot denotes differentiation with respect to time t. Setting,

$$x_1 = \xi\ ,\quad x_2 = \dot{\xi} \tag{8}$$

equation (7) can be written in normal form,

$$\begin{aligned}\dot{x}_1 &= x_2\\ \dot{x}_2 &= \Big\{\tau_0 n^2 + \\ &\quad + \sum_{i=1}^{N} f_i \sin\left[k_i x_1 - \omega_i t + \varepsilon_i^{(r)} + \varepsilon_{fi}\right] - \\ &\quad - \left(r_1 - \tau_1 n\right)x_2 - \left(r_2 - \tau_2\right)x_2^2 - r_3 x_2^3\Big\}\Big/\left(m - X_{\dot{u}}\right)\end{aligned} \tag{9}$$

where in the above $f_i = A_i RAO_i$.

4. APPLICATION

We select, as a case study, the tumblehome hull from the ONR topside series with $L = 154\ m$, $B = 18.8\ m$ and $T = 5.5\ m$. To test the applicability of the method in the problem considered, we first write system (9) for $N = 1$ (regular waves),

$$\begin{aligned}\dot{x}_1 &= x_2\\ \dot{x}_2 &= \left(m - X_{\dot{u}}\right)^{-1}\\ &\quad \Big[\left(\tau_1 n - r_1\right)x_2 + \left(\tau_2 - r_2\right)x_2^2 - r_3 x_2^3 + \\ &\quad + f\sin\left(k x_1 - \omega t + \varepsilon\right) + \tau_0 n^2\Big]\end{aligned} \tag{10}$$

We set the wave length and steepness values to $\lambda = L$ and $H/\lambda = 0.04$, respectively, where H the wave height. Deep water is assumed. For the calculation of the FTLE field, a grid is considered at $t_0 = 300\ s$ on a (x_1, x_2) domain. Integration time is set to $\tau = 45\ s$. The graph of the resulting field can be seen on the left part of figure 1. On the right part of the same figure, we visualize loci of points where the field surpasses a selected threshold of $0.85\mathrm{Max}\left(\Lambda_2\right)$. The emergent curves correspond to repelling LCSs over the interval $[t_0, t_0 + \tau]$.

To further examine the relevance of these structures with the stable and unstable manifolds of hyperbolic fixed points arising in the context of surf-riding in regular waves, we render (10) in autonomous form by considering the following transformations,

$$x_1 = x_1^w + ct\ ,\quad x_2 = x_2^w + c \tag{11}$$

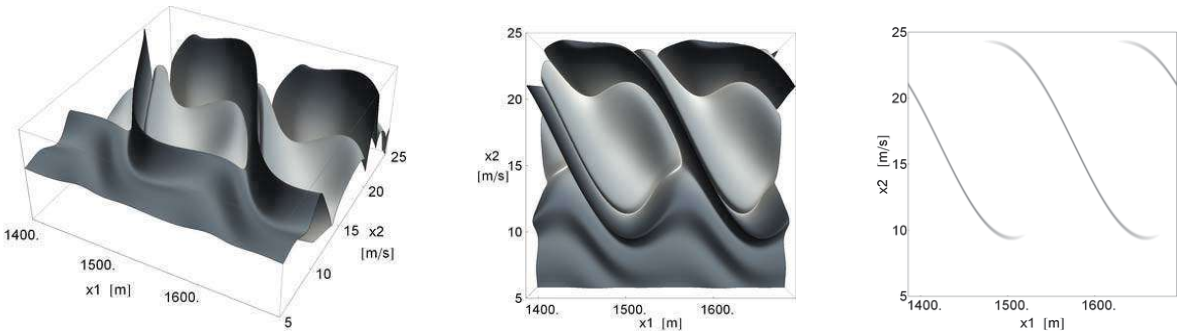

Figure 1 Harmonic excitation: The graph of the forward FTLE field over a (x_1, x_2) domain (left, middle). Loci of points where the field surpasses a selected threshold (right).

In the above, x_1^w and x_2^w is the longitudinal position and velocity, respectively, of the ship with respect to a frame located at a wave crest, translating with the wave celerity c.

Applying expressions (11) to system (10) we obtain, after rearranging, the following set of equations,

$$\begin{aligned}
\dot{x}_1^w &= x_2^w \\
\dot{x}_2^w &= \left(m - X_{\dot{u}}\right)^{-1} \\
&\left\{ \left[\tau_1 n - r_1 + 2c\left(\tau_2 - r_2\right) - 3r_3 c^2\right] x_2^w + \right. \\
&\quad + \left(\tau_2 - r_2 - 3r_3 c\right)\left(x_2^w\right)^2 - r_3\left(x_2^w\right)^3 + \\
&\quad \left. + f\sin\left(k x_1^w + \varepsilon\right) + g\left(c, n\right)\right\}
\end{aligned} \tag{12}$$

where,

$$\begin{aligned}
g\left(c,n\right) &= \tau_0 n^2 + \\
&+ \left(\tau_1 n - r_1\right)c + \left(\tau_2 - r_2\right)c^2 - r_3 c^3
\end{aligned} \tag{13}$$

It can be seen that system (12) does not depend (explicitly) on time. Stationary solutions can be obtained by setting the right hand side to be equal to zero and solving with respect to x_1^w and x_2^w. In the upper part of figure 2, a number of saddle points are identified and the unstable/stable manifolds are "grown" by integrating perturbed, with respect to the fixed points and along the eigendirections, initial conditions forward and backward in time. Wave length and nominal speed are set to $\lambda = L$ and $u_{nom} = 12.5\ m/s$. The figure on the left (right) correspond to a wave steepness of $s = 0.015$ $(s = 0.04)$.

We, consequently, consider system (10) and calculate, for the same settings, the forward $(\tau = 420\ s)$ and backward $(\tau = -240\ s)$ FTLE field at $t_0 = 0\ s$. LCSs are identified as in the case of figure 1. Results are presented in the lower part of figure 2; grey (black) lines correspond to repelling (attracting) LCSs. We note that the arrangement of the structures revealed is, substantially, identical to the arrangement of manifolds integrated from the saddle points. The only difference is that the former are translating with the wave celerity – as system (10) is expressed with respect to an earth-fixed frame.

We now introduce a second wave component i.e., system (9) is considered with $N = 2$. The length and steepness of the reference wave are set to $\lambda_1 = L$ and $s_1 = 0.04$. The parameters of the second wave component are fixed such that $\omega_2/\omega_1 = 0.91$ and $s_2/s_1 = 0.4$. Nominal speed is set to $u_{nom} = 12\ m/s$. FTLE fields are calculated at $258\ s$ and $282\ s$ (figure 3). As it can be noticed, LCSs seem to persist while their arrangement resembles, in a sense, to that observed in the regular case. This time though, the image is somehow "distorted" – as expected.

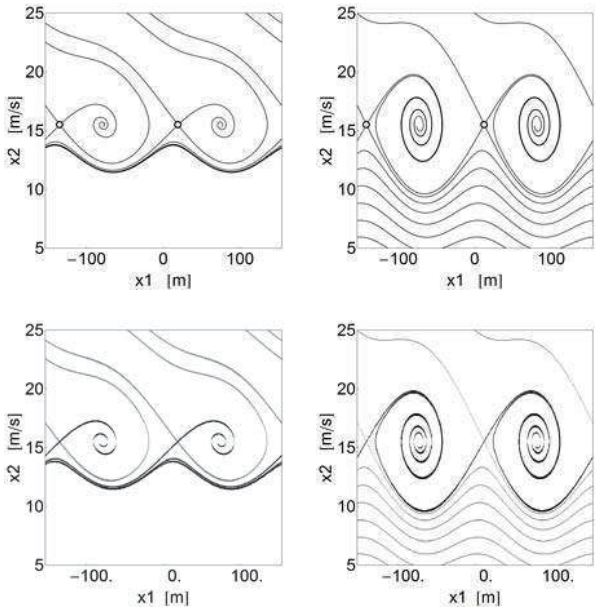

Figure 2 Top: Manifolds of hyperbolic points of (12). Bottom: LCSs of (10) obtained from forward (grey) and backward (black) FTLE fields.

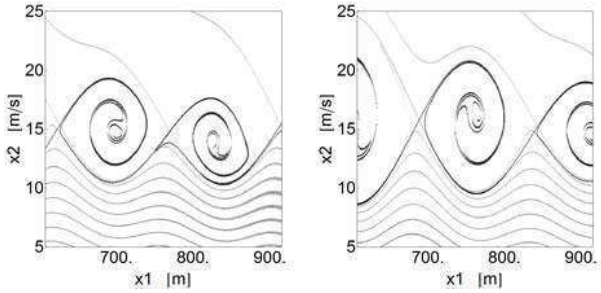

Figure 3 Bi-chromatic excitation: Attracting (black) and repelling (grey) LCSs.

The same procedure is repeated for the case of a JONSWAP spectrum with a peak period and significant height of $T_p = 10\ s$ and $H_s = 5.5\ m$, respectively. A frequency range of $0.5\omega_p$ is considered around the peak value ω_p and a 51-component wave is produced. Nominal speed is set to $u_{nom} = 12\ m/s$. Results are displayed in figure 4. As it can be seen, the arrangement of the identified structures appears to be fairly complicated.

Returning to the bi-chromatic scenario, we attempt, this time, to ascertain the organizing role of LCSs on the time-varying phase-flow. We set $\lambda = L$, $s_1 = 0.025$, $\omega_2/\omega_1 = 0.76$, $s_2/s_1 = 0.4$ and $u_{nom} = 12\ m/s$. In figure 5 a parcel of particles is integrated – these correspond to different initial conditions for the ship. The evolution of the parcel under the flow reveals different "long-term" behaviour of particle trajectories, as the former, after some time, splits in two. Some particles seem to respond in a surging-like manner (figure 5, particles on the left part of the last snapshot), while others seem to be engaged to surf-riding (same snapshot, right part).

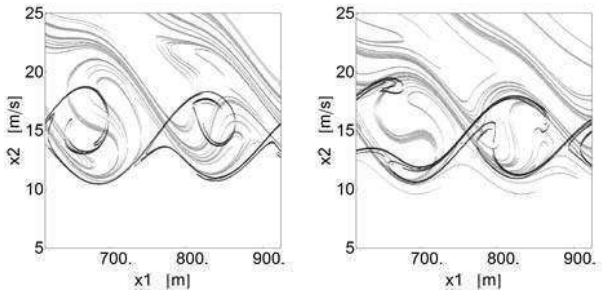

Figure 4 Attracting (black) and repelling (grey) LCSs for the case of a JONSWAP spectrum (51 wave components).

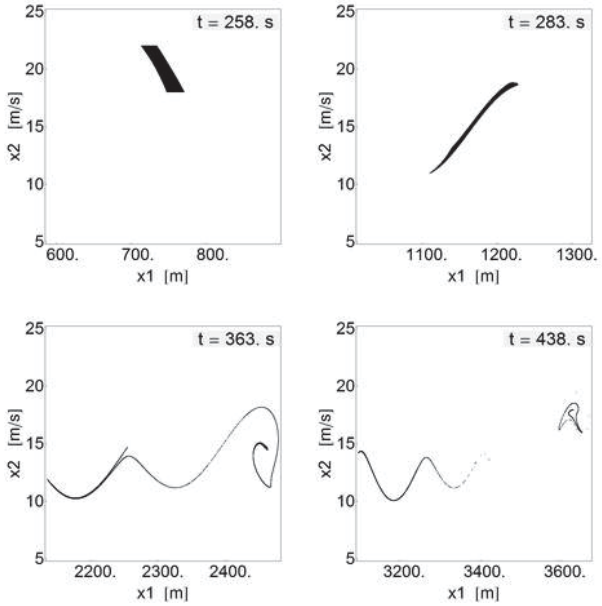

Figure 5 Bi-chromatic excitation: Integration of a dense patch of initial conditions reveals qualitatively different "long-term" behaviour of particle trajectories.

We keep the same setting and calculate the FTLE field on a domain containing the initial conditions ($t = 258\ s$). It seems that the "sus-

pect" for the situation depicted above can be identified among the repelling LCSs of the phase flow. Specifically, the repelling LCS associating with the hyperbolic trajectory passing near (790,16) at time $t = 258\ s$ (figure 6, snapshots on the left), acts as a transport barrier between regions of the flow with distinct dynamics. In fact, particles travel along this repelling structure towards the hyperbolic trajectory, where they are redirected towards different branches of the attracting LCS correlating with the same trajectory (figure 6, last three snapshots, top and bottom row).

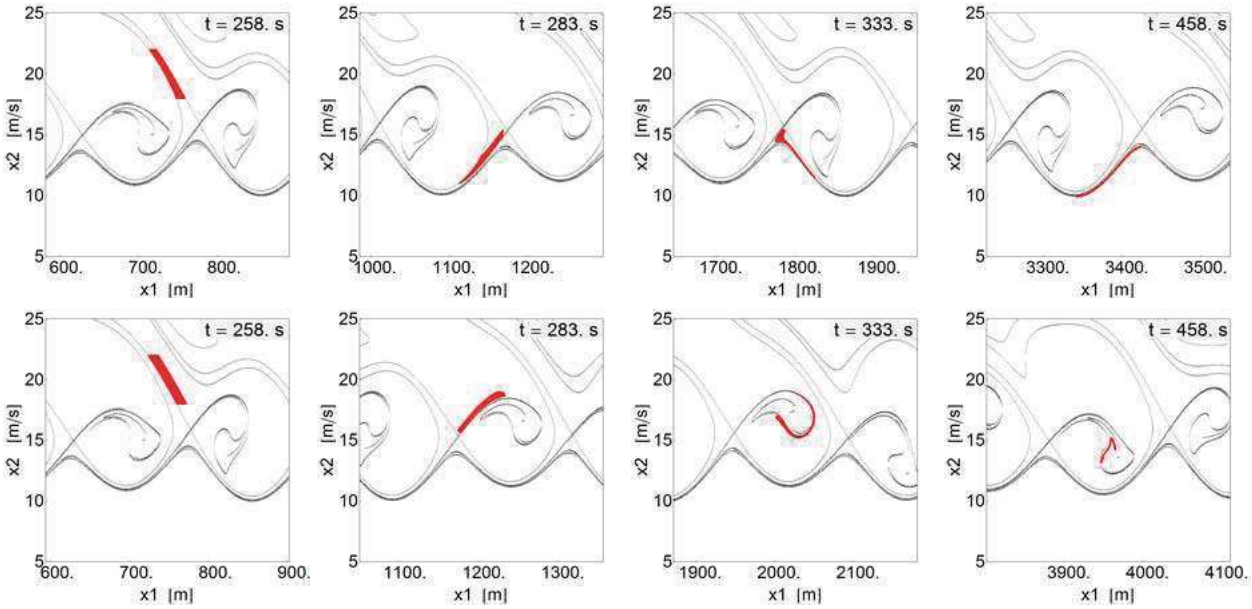

Figure 6 Same setting as in figure 5. Advection of two adjacent phase-particle parcels (red); integration of 91.000 and 118.000 (approx.) initial conditions, top and bottom row respectively.

Lastly, a bi-chromatic scenario is considered, with the frequency and steepness ratio of the two related wave components set to $\omega_2/\omega_1 = 0.93$ and $s_2/s_1 = 0.5$, respectively. The reference wave has been chosen such that $\lambda_1 = L$ and $s_1 = 1/30$, while nominal speed is set to $u_{nom} = 12\ m/s$.

We differentiate (9) with respect to time to obtain the acceleration field $a = (\ddot{x}_1, \ddot{x}_2)$ – the use of this term is justified from the fact that one can interpret (9) as a velocity field on the phase plane. Our objective is to track critical points of a i.e., points where the acceleration vector vanishes. In Spyrou et al. (2014b) it has been conjectured that certain critical points of this field correlate with surf-riding events. Furthermore, in Spyrou et al. (2015) it has been argued that critical points of a moving along paths that "resemble" to solutions of (9) seem to mark regions in the extended phase space where ensembles of trajectories are engaged to surf-riding.

In figure 7, a simulation corresponding to the aforementioned scenario can be seen (red line). Distance is measured from amidships (x-axis) while u-axis refers to velocity as measured by an on-shore observer. Three critical points of the acceleration field have been detected at around $t = 220\ s$ (these have been selected as they are related to the calculated trajectory; one could find more critical points at different space-time intervals). Their paths (grey and black lines) have been computed using the Feature Flow Field method (Theisel & Seidel 2003). In the same figure, we have included sections depicting LCSs that have been identified on phase-space windows around the ship at selected time instants. There seems to be a strong correspondence between the paths

of two critical points (denoted with grey lines) and hyperbolic trajectories revealed via the FTLE fields. The third critical point, on the other hand, appears near the core of an attracting LCS, in a region of the phase flow where a surf-riding state can be revealed (Spyrou et al. 2015). It is noted that for the considered arrangement, this would be a periodic trajectory with an attracting character.

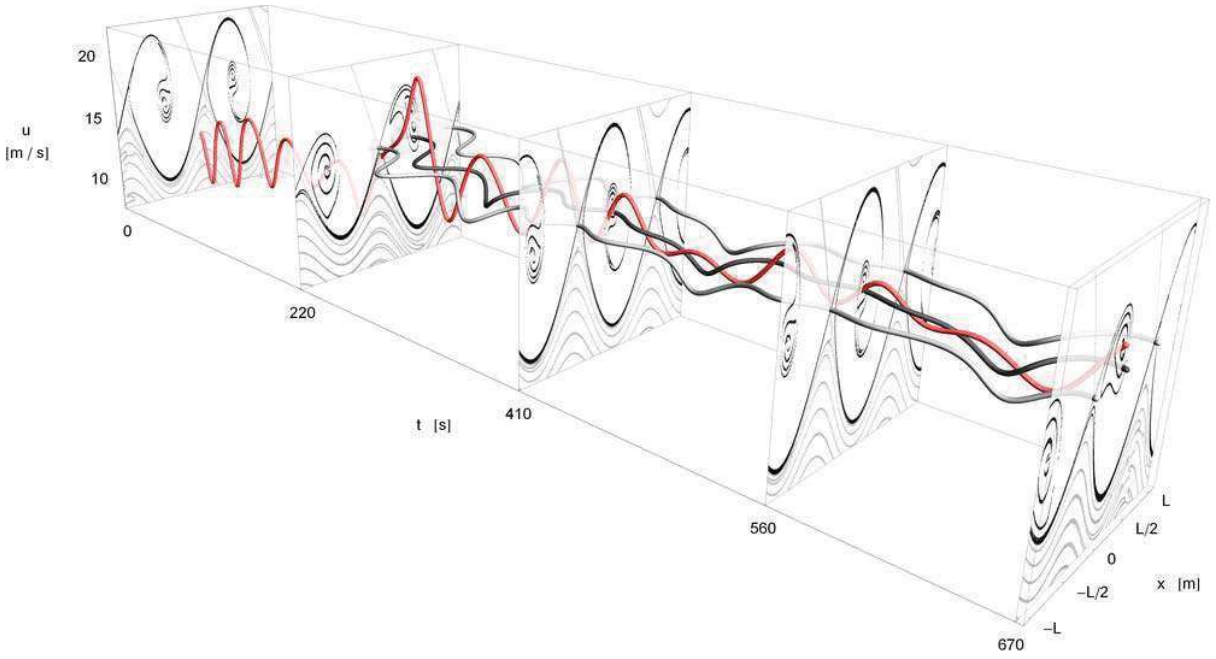

Figure 7 Bi-chromatic excitation: Ship trajectory (red line), LCSs at selected time instants and paths of three critical points of the acceleration field (black and gray lines).

5. CONCLUDING REMARKS

Methods for gaining insight into the dynamics of ship surge motion in astern multichromatic seas are introduced. Specifically, an identification method for Lagrangian Coherent Structures (LCSs) is applied on the phase flow defined by the surge equation of motion. It is based on a well-known scheme with a wide range of applications in the literature, which involves the calculation of the spatial distribution of the largest finite-time Lyapunov exponent (FTLE). Through the FTLE field, LCSs i.e., influential material lines shaping the pattern of the time-dependent flow, were obtained. Their role as phase-flow organizing structures was examined. It was found that, for the case of a bi-chromatic scenario, LCSs can help to understand the evolution of ensembles of initial conditions, by providing the location of transport barriers, as well as the final destinations of particle trajectories.

Furthermore, the Feature Flow Field method was implemented for the tracking of features, corresponding to elements of the zero set of the acceleration field defined by the surge equation of motion. Results obtained from the tracking of such features and the LCSs identification procedure were combined. It has been shown that the paths of certain features correlate to hyperbolic trajectories of the surge equation, while others to trajectories with attracting character that seem to evolve in the core of specific branches of attracting LCSs.

6. ACKNOWLEDGEMENTS

The calculation and testing of LCSs for surging and surf-riding behaviour described in this paper have been funded by the Greek General Secretariat of Research and Technology under the General Program ARISTEIA I (contract reference number GSRT-252). The work regarding the feature tracking method applied in Section 4 has been funded by the Office of Naval Research, ONRG grant number N62909-13-1-7, under Dr. Ki-Han Kim, Dr. Tom Fu and Dr. Woei-Min Lin.

7. REFERENCES

Belenky, V., Spyrou, K., & Weems, K., 2012, "Evaluation of the probability of surf-riding in irregular waves with the time-split method", Proceedings of 11th International Conference on the Stability of Ships and Ocean Vehicles, Athens, Greece, pp. 29-37.

Haller, G. and Yuan, G., 2000, "Lagrangian coherent structures and mixing in two-dimensional turbulence", Physica D, 147, pp. 352-370.

Haller, G., 2011, "A variational theory of hyperbolic Lagrangian Coherent Structures", Physica D, 240, pp. 574-598.

Kan, M., 1990, "Surging of Large Amplitude and Surf-riding of Ships in Following Seas", Selected Papers in Naval Architecture and Ocean Engineering, The Society of Naval Architects of Japan, 28.

Shadden, S. C., 2011, "Lagrangian Coherent Structures", Transport and Mixing in Laminar Flows: From Microfluidics to Oceanic Currents, Roman Grigoriev, Ed., Wiley-VCH.

Spyrou, K., 1996, "Dynamic instability in quartering seas: The behaviour of a ship during broaching", Journal of Ship Research, SNAME, 40, No 1, pp. 46-59.

Spyrou, K., Belenky, V., Themelis, N., & Weems, K., 2012, "Conditions of surf-riding in an irregular seaway", Proceedings of 11th International Conference on Stability of Ships and Ocean Vehicles, Athens, Greece, pp. 323-336.

Spyrou, K., Belenky, V., Themelis, N., & Weems, K., 2014a, "Detection of surf-riding behaviour of ships in irregular seas", Nonlinear Dynamics, DOI 10.1007/s11071-014-1466-2.

Spyrou, K., Belenky, V., Reed, A., Weems, K., Themelis, N., Kontolefas, I., 2014b, "Split-Time Method for Pure Loss of Stability and Broaching-To", Proceedings of 30th Symposium on Naval Hydrodynamics, Hobart, Tasmania, Australia.

Spyrou, K., Themelis, N., Kontolefas, I., 2015, "Development of Probabilistic Models for Evaluating the Dynamic Stability and Capsizing Tendency of Naval Vessels with Respect to Broaching-to", Technical Report to the Office of Naval Research (2015), ONRG grant number: N62909-13-1-7.

Theisel, H., Seidel, H-P., 2003, "Feature flow fields", Data Visualization 2003, Proc. VisSym 03, 2003, pp. 141-148.